JOURNAL OF PROPULSION AND POWER
Vol. 12, No. 5, September–October 1996

Semiempirical Predictions and Correlations of CO Emissions from Utility Combustion Turbines

C. S. Connors,* J. C. Barnes,† and A. M. Mellor‡
Vanderbilt University, Nashville, Tennessee 37235

Semiempirical models for gas-turbine combustor emissions distinguish between the dominant subprocesses of combustion related to pollutant emissions. They assign characteristic times, which are based on combustor geometry, fuel characteristics, and operating conditions, to these subprocesses. Linear ratios of these characteristic times, or of sums of the times weighted with empirical constants, are proportional to the emissions indices of oxides of nitrogen and of carbon monoxide (CO). The capability of a semiempirical model to predict and correlate CO emissions from two heavy-duty, dual-fuel (natural gas and fuel oil) diffusion flame combustors without inert injection is assessed. The model is termed the characteristic time model. Since the characteristic time model had not been used to correlate or predict CO emissions from stationary, heavy-duty combustors prior to this study, application of the models to the heavy-duty emissions data was not expected to, and did not yield acceptable predictions or correlations. Thus, modification of the characteristic time model was performed. A new algorithm determines the CO oxidation quench position in the combustor and provides a reasonable correlation of the CO data.

Nomenclature

b = y-intercept of a linear equation
COEI = carbon monoxide emissions index, g CO/kg fuel
Da = Damköhler number
Da^* = Damköhler number modified for evaporation effects
d_{comb} = diameter of the combustor, m
d_0 = Sauter mean diameter
E = activation energy, cal/gmol
$[i]$ = concentration of species i
k = specific reaction rate coefficient
k_{CO} = empirical coefficient for droplet evaporation
l_{CO} = characteristic length for CO oxidation, m
l_{comb} = combustor length, distance downstream from the fuel injector tip to the exit plane of the combustor, m
l_{pri} = primary length, distance downstream from the fuel injector tip to the centerline of primary air addition holes, m
l_{quench} = quench length, distance downstream from the fuel injector tip to the quench location, m
l_{sec} = secondary length, distance downstream from the fuel injector tip to the centerline of secondary air addition holes, m
M = molecular weight, g/gmol
m = slope of a linear equation
$\dot{m}$ = mass flow rate, kg/s
$\dot{m}_a$ = total combustor airflow rate, kg/s
NO_x = oxides of nitrogen, NO and NO_2
NO_xEI = oxides of nitrogen emissions index, g NO_x as NO_2/kg fuel
P = pressure, atm
R = universal gas constant, cal/kgmol K
r = correlation coefficient
T = temperature, K
$\bar{T}$ = average of combustor inlet and exit temperatures, K
V_{ref} = reference velocity, m/s
x = independent variable in linear equation
β = fuel droplet evaporation coefficient, m^2/s
σ_y = standard deviation of the y values for the observed values of x
τ_{CO} = characteristic time for CO oxidation, $10^{-3}\exp(10{,}760/R\bar{T})$, ms
τ^*_{CO} = characteristic time for CO oxidation incorporating the primary zone equivalence ratio, $10^{-3}\exp(10{,}760/R\bar{T})/\phi_{pz}$, ms
τ_{eb} = evaporation time, ms
$\tau_{sl,CO}$ = residence time in the shear layer where CO oxidation occurs, ms
ϕ = fuel–air equivalence ratio

Subscripts
a, air = air
CO = carbon monoxide
exh = exhaust
fuel = fuel
in = inlet value
pz = primary zone
s = value at liquid saturation point or drop surface
0 = initial condition

Received June 8, 1995; revision received May 5, 1996; accepted for publication May 10, 1996.

*Undergraduate Research Assistant, Department of Mechanical Engineering. Student Member AIAA.
†Graduate Research Assistant, Department of Mechanical Engineering. Student Member AIAA.
‡Centennial Professor of Mechanical Engineering. Associate Fellow AIAA.

Introduction

STRICTER emissions standards for most combustion devices, including gas turbines, have been mandated in recent years. Accordingly, industry is designing and implementing low-emissions hardware. An accurate design model would reduce both time and cost of the developmental process. In addition, an accurate emissions model can substitute for neural networks and continuous emissions monitors or verify actual emissions data when a monitoring system is available.[1]

The modeling used to evaluate combustors can be divided into three levels: 1) numerical, 2) semiempirical, and 3) empirical. While computational fluid dynamic codes are being used more widely to approximate flowfields and temperature

patterns within combustors, they do not, in general, provide quantitative predictions of gaseous emissions. At the other end of the spectrum, completely empirical models rely only on measured data and are applicable only to the device for which they were developed.

Semiempirical models for combustor emissions fall between these extremes. Characteristic times are assigned to fuel spray evaporation (if applicable), pollutant chemical kinetics, and combustor fluid mechanics and are calculated in terms of geometry, fuel characteristics, injector type, and operating conditions. Emissions indexes of specific pollutants, namely, oxides of nitrogen (NO_x) and carbon monoxide (CO), can be shown proportional or inversely proportional to Damköhler numbers formed from these characteristic times.[2]

In this work, a semiempirical model is used to predict and correlate dry CO emissions data from two heavy-duty, dual-fuel diffusion flame combustors. The model is named the characteristic time model (CTM), and was developed by Tuttle et al.[2] This model was calibrated primarily with emissions data from aircraft engine combustors and has not been used with measurements from the power-generation engines of this study. As will be seen, operational differences exist between aeroengine and heavy-duty combustors that affect the performance of the model. To account for the differences, the CTM is modified and optimum correlations of the data are achieved.

Combustor Information

The two combustors involved in this study, termed combustors A and B, are diffusion flame combustors of the canannular or tuboannular type and have dual-fuel capability (natural gas or fuel oil). The combustors are used in stationary gas-turbine engines that generate power in the 100–150 MW range. Injection of water or steam into the combustor is used for NO_x reduction, but is not considered here.

Emissions and operating conditions data were provided by the respective manufacturers. The data supplied for combustor A included eight without inert injection, four using natural gas and four using fuel oil. For combustor B, 35 data without inert injection were reported. These included 23 natural gas points at two different inlet guide vane (IGV) settings and 12 fuel oil points at one IGV setting. The combustor A data are measurements taken from one test run, whereas combustor B data are averages developed from multiple tests. No statistical information was provided to the authors by either manufacturer regarding the accuracy of the data.

The reported exhaust concentrations include NO_x and CO. Semiempirical predictions and correlations of the NO_x emissions from these combustors have been completed (see Newburry and Mellor[3] for data without inert injection and Newburry and Mellor[4] for data with water/steam injection). The thermochemical code STANJAN[5] was used for the calculation of equilibrium adiabatic flame temperatures. The fuel files used by STANJAN were compiled for each fuel using information provided by the manufacturers. Since the reported data for combustor B were averaged values, the fuel files constructed for this combustor contained average fuel compositions, as one specific composition was not available for either fuel-oil or natural-gas firing.

For data generated using fuel oil, estimated evaporation times were calculated using the d^2 law of Godsave[6]:

$$\tau_{eb} = d_0^2/\beta_{conv} \tag{1}$$

where d_0, the initial droplet diameter, is taken as the spray Sauter mean diameter (SMD) and β_{conv} is the evaporation coefficient. Forced convection effects are accounted for in the CTM with an empirical correlation by Frössling[7] in accordance with assumptions made by Leonard and Mellor.[8]

The SMD has the same ratio of volume-to-surface area as the spray as a whole. For combustor A, Sauter mean diameters were reported for each datum. They were not provided for the combustor B injector, and therefore were calculated using an empirical correlation by Elkotb et al.,[9] which was updated by Lefebvre.[10]

Although combustors are designed similarly for aircraft and stationary engines, operating conditions vary between the two. Stationary cycles are usually limited to lower compressor pressure ratios to increase hot section durability. In addition, nonaeroderivative combustors operate with nearly constant inlet airflow rate at all power settings, whereas in aircraft combustors a constant reference velocity is generally maintained. As a result, power-generation combustors operate over a much wider range of overall equivalence ratios than do aircraft combustors. The greater range of ϕ implies that stationary combustors experience wider turndown ratios, the ratio of maximum-to-minimum equivalence ratio from full-power-to-idle. Table 1 includes turndown ratios for all engines correlated previously both in the CO and the combustion efficiency[8] CTMs. The engines are grouped by application and it is seen that, with the exception of the GT-309 that uses a regenerative cycle, all of the nonstationary engines are limited to a turndown ratio of 2 or less. In contrast, the turndown ratios for the stationary combustion turbines are considerably larger.

As a further demonstration of differences between the two types of cycles and combustors, a Verkamp plot[11] of COEI vs the oxides of nitrogen emissions index (NO_xEI, g NO_x as NO_2/kg fuel), both on logarithmic axes, is shown in Fig. 1. Note that 1-g CO/kg fuel equals approximately 19-ppmvd (parts per million by volume, dry) CO at 15% O_2, and the conversion for NO_xEI is about 11-ppmvd NO_x at 15% O_2 per g NO_2/kg fuel (precise values depend on equivalence ratio). Included in the figure is a reconstruction of the tradeoff for conventional combustors,[11] measured data for the TF41,[12] F101,[13] and JT9D[14] aircraft combustors, and an outlined region where the combustors A and B data fall. As seen, the data for the aircraft combustors agree, for the most part, with the region of Verkamp's data.

While the areas of the data for combustors A and B coincide, CO emissions extend over a wider range because of the larger heavy-duty turndown ratio, and the range of NO_x values is more narrow than that of the aeroengines. Peak emissions of CO and NO_x are lower for the stationary combustors because of the larger residence times and lower peak cycle pressures, respectively. The significantly lower minimum CO values are also attributed to the larger size of the heavy-duty combustors. The other major difference between the emissions characteristics of the two types of combustors is the slope of the tradeoff: for all burners, higher NO_x leads to lower CO, and vice versa, but for combustors A and B the trend is constrained to a narrower range of NO_x emissions because of the lower values of compressor pressure ratio. The wider range of CO emissions shown here foreshadows difficulties with the existing CO CTM.

Table 1 Ratio of the maximum-to-minimum fuel/air equivalence ratio for several turbine combustors and fuels

Combustor	Fuel	ϕ_{max}/ϕ_{min}
Fixed and rotary wing aircraft engines		
T-63	JP4	1.8
F101	Various liquids	2.0
TF41	Various liquids	1.6
JT9D	Jet A	2.0
Vehicular engines		
AGT-1500	Various liquids	1.9
GT-309	DF-2	3.7
Stationary engines		
Combustor A	Natural gas	2.9
Combustor A	Fuel oil	3.3
Combustor B	Natural gas	3.6
Combustor B	Fuel oil	4.1

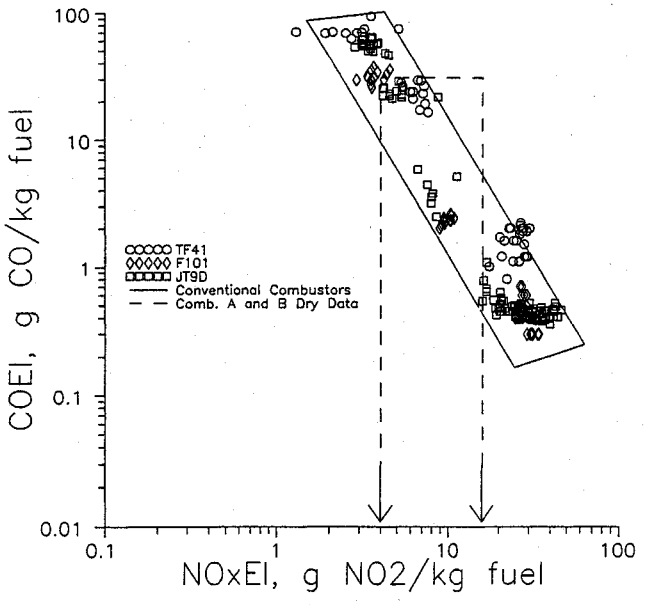

Fig. 1 Dry emissions tradeoff range for heavy-duty combustors A and B, fired on gas or oil, compared with the conventional combustor range of Verkamp et al.[11] Data from the TF41, F101, and JT9D aeroengine combustors[12-14] are superimposed.

Characteristic Time Model for CO Emissions

The CTM utilizes characteristic times for a gas-turbine diffusion flame combustor. The characteristic times are order of magnitude estimates of dominant subprocesses and are calculated from combustor geometry, operating conditions, and fuel and injector properties. Thus, in theory, the model can be applied successfully to different combustors without altering the respective characteristic time expression.

In the CTM, the correlating parameter for CO emissions index takes the form of an inverse Damköhler number, or a characteristic kinetic time divided by a characteristic fluid time.[15] As will be seen, the CTM accounts for finite rate evaporation by adding an evaporation time to the kinetic time. The Damköhler number including the drop lifetime is denoted $D\tilde{a}^*$. To provide quantitative emissions predictions, model constants m and b must be determined by calibration with experimental data, where

$$\text{COEI (g CO/kg fuel)} = m \times D\tilde{a}^{*-1} + b \tag{2}$$

Two versions of the characteristic time model are summarized in Table 2. Included are the model equations, the recommended best-fit slopes, m, and y-intercepts, b, and the empirical weighting factor k_{CO}, which multiplies τ_{eb} when heterogeneous effects are important. The value of k_{CO} has no physical significance as each characteristic time is an order of magnitude estimate.

The characteristic time model for CO was first developed[2] for disc-in-duct laboratory flameholders. It was then extended to gas-turbine combustors.[16-18] The model has not been used previously with CO emissions from heavy-duty turbine combustors.

The methodology behind the CTM for CO is as follows. Carbon monoxide is formed during an intermediate step in the combustion reaction kinetics. After it is produced, if the pollutant remains at an adequately high temperature for a long enough period of time, it begins to oxidize by combining with hydroxyl free radicals (OH). Therefore, the amount of CO emitted by a combustor is inversely proportional to the residence time of the pollutant in the CO burnout zone before quenching of the oxidation occurs. Tuttle et al.[2] named this characteristic time $\tau_{sl,CO}$.

Table 2 Characteristic time model equations for COEI, including model constants, modified for finite rate evaporation

Model	m	b	$D\tilde{a}^{*-1}$	k_{CO}
Washam	35	0	$\tau_{CO}/\tau_{sl,CO}$	—
Leonard	32.2	−0.25	$(\tau_{CO} + k_{CO}\tau_{eb})/\tau_{sl,CO}$	0.04

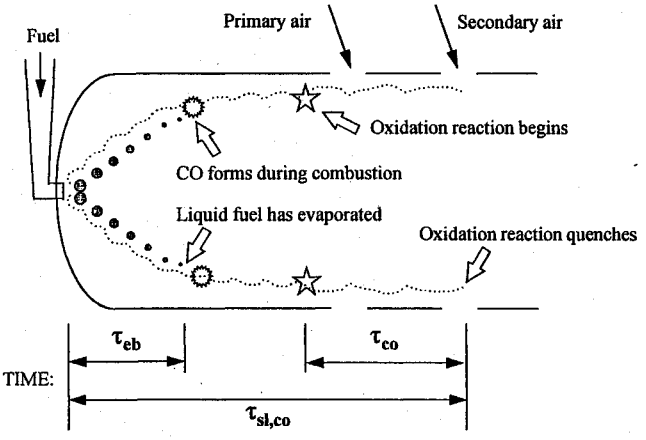

Fig. 2 Qualitative diagram of combustion subprocesses relating to CO emissions and associated characteristic times.

The step in the chemical process where CO oxidizes to CO_2 is shown by the reaction:

$$CO + OH \rightarrow CO_2 + H \tag{3}$$

By applying the law of mass action to the forward reaction only, the following expression is obtained:

$$\frac{d[CO]}{dt} = -k[CO][OH] \tag{4}$$

Tuttle et al.[2] assumed that [OH] is in steady state within the high-temperature eddies in which CO oxidation occurs, and by integrating Eq. (4) over the eddy lifetime $\tau_{sl,CO}$, they obtained a first-order expression for COEI after expansion of the resulting exponential in a power series and retaining only the term inversely proportional to Da. Heterogeneous evaporation delays because of liquid fuels are added to the kinetic delay, as shown in Table 2. In total, the CTM is based then on three characteristic times: 1) the kinetic time for CO to oxidize to CO_2 (τ_{CO}), 2) the time it takes for a liquid fuel droplet of mean size to evaporate (τ_{eb}), and 3) the length of time before quenching a CO oxidizing eddy ($\tau_{sl,CO}$). Figure 2 is a schematic of the overall CO formation/oxidation process for quenching at the secondary holes.

The kinetic time for τ_{CO}, takes the form of an inverse Arrhenius relation. It is defined as

$$\tau_{CO} = 0.001 \exp(10{,}760/R\bar{T}), \text{ ms} \tag{5}$$

where the pre-exponential factor 0.001 was chosen so that τ_{CO} is on the order of milliseconds. The activation energy E_{CO} (10,760 cal/gmol) was determined from Arrhenius plots of combustor CO emissions data. It is based on the average of the combustor inlet and exhaust temperatures

$$\bar{T} = \tfrac{1}{2}(T_{in} + T_{exh}), \text{ K} \tag{6}$$

where T_{exh} is the calculated adiabatic flame temperature at the overall combustor equivalence ratio. The residence time in the flow where CO oxidation occurs is defined as

$$\tau_{sl,CO} = l_{CO}/V_{ref} \tag{7}$$

where V_{ref} is based on the maximum combustor cross-sectional area:

$$V_{ref} = \frac{\dot{m}_a RT_{in}}{P_{in} M_a (\pi/4) d_{comb}^2} \tag{8}$$

Comparisons of $\tau_{sl,CO}$ with experimental length scale and turbulent velocity data[19-21] indicate that $\tau_{sl,CO}$ appropriately describes integral scale vortex dissipation in the shear layer and wake region behind various flameholder geometries.

The characteristic length for CO oxidation is the following combination of quench length and combustor diameter:

$$l_{CO}^{-1} = l_{quench}^{-1} + d_{comb}^{-1} \tag{9}$$

The quench length l_{quench} for CO is the distance downstream of the tip of the fuel injector at which CO stops oxidizing to carbon dioxide. This termination of the oxidation reaction is referred to as CO quenching and occurs when eddy temperature becomes too low, most likely near the combustor walls, where air is added through various openings. Thus, the quench length is the axial distance to the air addition site that causes this temperature drop.

In the CTM, CO emissions are inversely proportional to l_{CO}. Thus, an accurate estimate of l_{quench} is imperative to the success of the CTM in predicting CO emissions, since d_{comb} is also evaluated at the quench length. Three definitions of l_{quench} have been used previously. The first, as used by Mellor,[16] is purely empirical and will not be considered here. In the second method[18] l_{quench} is defined as the length from the tip of the fuel injector to the air addition site that causes the local, fully-mixed equivalence ratio to fall below 0.2. Finally, Leonard and Mellor[8] defined the quench length as l_{sec} if $\phi_{pz} > 1.0$, and otherwise as l_{pri}. The primary zone equivalence ratio ϕ_{pz} for Leonard's rule is computed using the primary air, any swirler air, and dome cooling air. These latter two methods are referred to as Washam's rule and Leonard's rule.

The different predicting equations presented in Table 2 for the CTM correspond to the two quench length definitions. Only Leonard's rule includes droplet evaporation effects. The evaporation time is multiplied by a recommended k_{CO} of 0.04 and is then added to τ_{CO} in the numerator of the model equation.

Original CO Emissions Predictions and Correlations

Of the two methods for determining quench length in the characteristic time model, Washam's rule provides the better results. Figure 3 is the model equation graph for the CO CTM using Washam's rule to evaluate quench length. The graph presents measured COEI values (symbols) for both combustors, fired on either gas or oil, vs the CTM model equation. Data at full load are located near the origin and at idle in the upper right-hand corner. It is noted that CO emissions are higher for natural gas as fuel than for no. 2 oil. The model prediction (using m in Table 2) is given by the dashed line, while the least-squares fit is shown by the solid line and the equation in the figure. The quality of the correlation (solid line) is reasonable with a correlation coefficient of 0.97 and a standard deviation of 1.09 g/kg, equal to the magnitude of the negative y-intercept. The model slightly overpredicts the CO emissions from both combustors. However, if the fuel oil and natural gas data are correlated separately, excellent linear correlations are obtained: the fuel oil data exhibit a correlation coefficient of 0.99 and a standard deviation of 0.40 g/kg, while the natural gas data are characterized by $r = 0.99$ and $\sigma_y =$ 0.89 g/kg. Even more important is that, with a best-fit slope of 34.53 g/kg, the natural gas data examined by themselves agree with Mellor and Washam's[18] recommended slope of 35 g/kg (albeit with a negative y-intercept). However, the fuel-oil data are significantly overpredicted by the CTM that neglects finite rate evaporation since the correlation slope is 23.68 g/kg (see Table 2). The Leonard and Mellor[8] approach that adds the evaporation delay to the CO oxidation time, as shown in Table 2, will displace the fuel-oil data (with positive values of τ_{eb}) farther to the right of the natural gas data when graphed in a similar manner to Fig. 3.

The agreement between the natural gas result and the CTM equation developed previously[18] for liquid-fueled aircraft and vehicular combustors of significantly smaller scale indicates that similar portions of the combustor flowfield are responsible

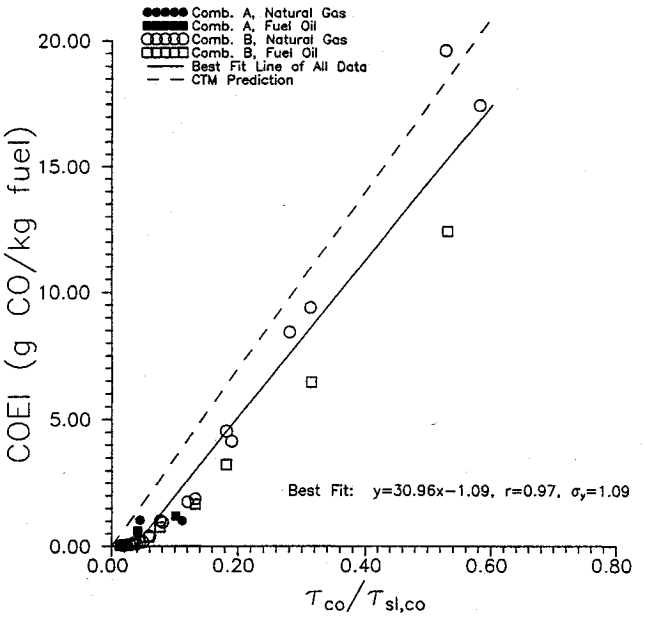

Fig. 3 Characteristic time model equation graph of combustors A and B CO data, without inert injection, using Washam's rule for l_{quench}.

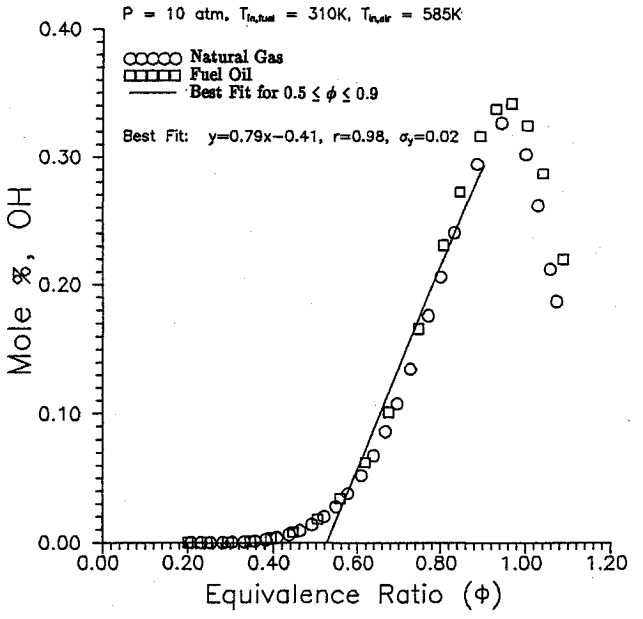

Fig. 4 Equilibrium hydroxyl concentration as a function of equivalence ratio for typical heavy-duty combustor inlet conditions for two fuels. The solid line is a linear least-squares fit in the $0.5 \leq \phi \leq 0.9$ range.

for CO emissions. These regions are generally agreed to occur at outer boundaries of the shear layer surrounding the recirculating flow in the primary zone.[22] In contrast, since the heavy-duty combustor fuel-oil CO emissions are overpredicted by the same model, one interpretation is that CO oxidation reactions occur at somewhat higher temperatures for oil firing (oil is generally injected more closely to the burner centerline than gas). In fact, it was found that increasing the average temperature in τ_{CO} by only 55 K collapsed the oil and gas data. However, without this empirical, a posteriori modification, it is concluded that the CTM is unable to correlate the data for the two fuels together.

Connors et al.[23] also investigated two additional semiempirical models for CO emissions, but space limitations prevent inclusion of the results here. Both Lefebvre[24] and Rizk and Mongia[25] worked with aircraft engine data to obtain model constants, and, for reasons discussed in the Combustor Information section, predictions of CO emissions indices with these models were generally inferior to those for the CTM shown in Fig. 3. Consequently, further efforts to develop an adequate correlation for power-generation machines were focused on the characteristic time model.

Modification of the CTM for CO Emissions

The observations resulting from Table 1 and Fig. 1 suggested that semiempirical models for CO emissions calibrated with aircraft engine data would not accurately predict CO levels emitted by heavy-duty combustors, as the results in Fig. 3 verify. However, the encouraging findings just discussed indicated model modifications with the CTM could prove fruitful. Accordingly, first the wider turndown ratio range in Table 1 is addressed by imitating the variation of OH radical concentration in Eq. (3) with primary zone equivalence ratio instead of assuming it constant,[2] and second, the incorrect modeling of effects of finite rate fuel evaporation is changed through reconsideration of the combustor processes with oil firing and development of a new quench length criterion.

From Eq. (4) it is obvious that the CO CTM would be improved if the concentration of hydroxyl in the CO oxidation region were included explicitly in the model equation. Tuttle et al.[2] realized that this information is unavailable for most combustors and thus simply assumed hydroxyl is in steady state, an assumption that was continued with some success.[8,18] As an index of variation of the actual hydroxyl concentration, an engineering approximation of improved accuracy to the

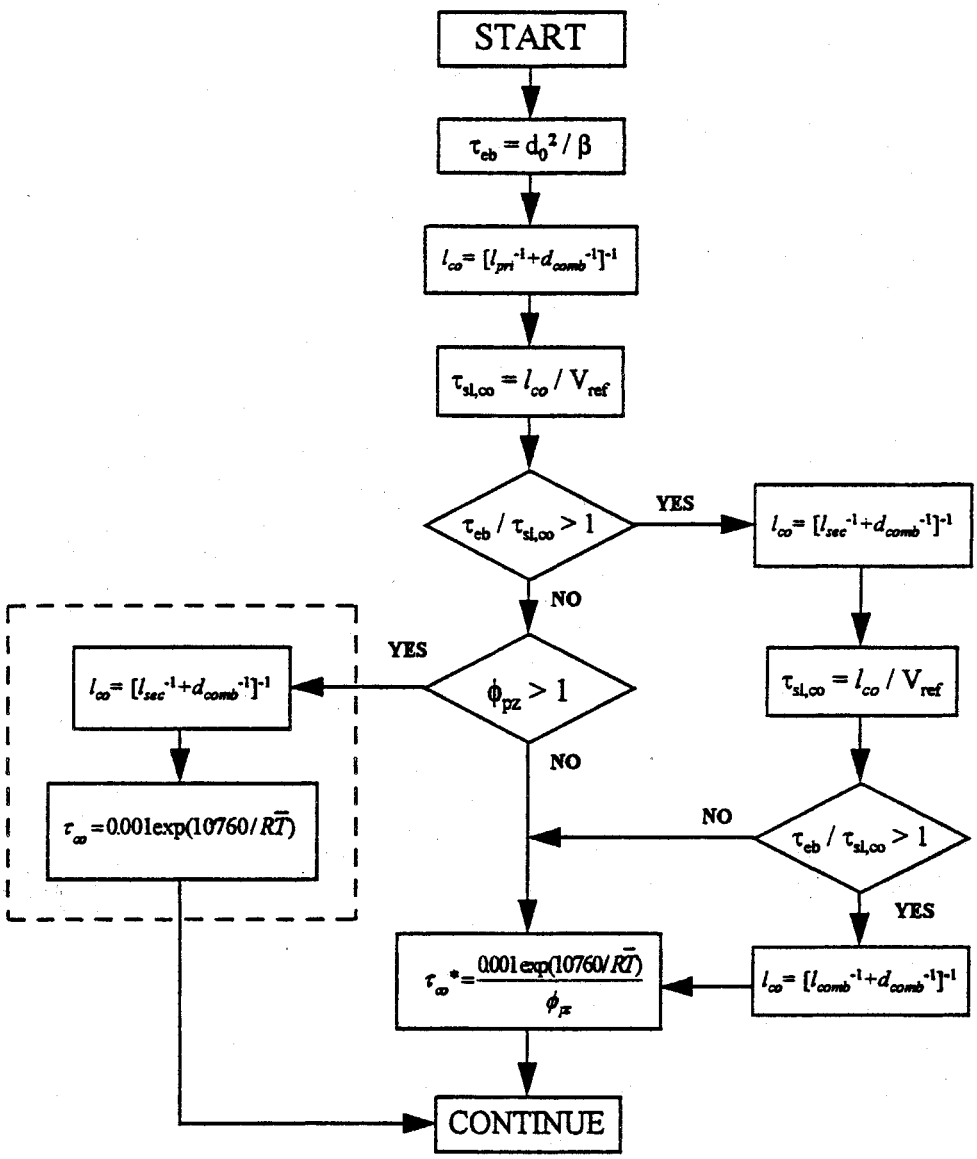

Fig. 5 New algorithm flowchart for evaluating CO quench length and characteristic CO oxidation kinetic time in CTM correlations for heavy-duty combustors fired on gas or oil.

steady-state assumption is substitution of the equilibrium value of hydroxyl concentration computed for the primary zone. Calculations were made with STANJAN[5] using both natural gas and fuel oil at a range of lean equivalence ratios for typical heavy-duty combustor inlet conditions. These calculations demonstrated that there is a first-order dependence of equilibrium hydroxyl concentration on primary zone equivalence ratio when the primary zone is lean ($\phi_{pz} < 1$), as shown in Fig. 4.

Leonard and Mellor[8] also found lean primary zone performance an important factor in the combustion process and incorporated ϕ_{pz} into their CTM for combustion efficiency. Following Leonard and Mellor,[8] ϕ_{pz} was also added to the kinetic time for CO formation:

$$\tau^*_{CO} = \tau_{CO} \quad \text{if} \quad \phi_{pz} > 1.0 \tag{10}$$

$$\tau^*_{CO} = \tau_{CO}/\phi_{pz} \quad \text{if} \quad \phi_{pz} < 1.0 \tag{11}$$

where for the CO CTM primary zone airflow is estimated as any swirler air, all dome air, all film air entering upstream of the primary holes, and one-half of the primary air.

The OH, or equivalence ratio, dependence was not required for the aeroderivative combustors with the smaller turndown ratios because they operate over a smaller range of ϕ and ϕ_{pz}, as suggested by Table 1. Therefore, the difference between the maximum and minimum OH concentrations is much smaller than it is for the heavy-duty combustors.

Although the use of τ^*_{CO} was expected to improve the CTM for the CO correlation, it does not distinguish between natural gas and fuel-oil firing. Leonard and Mellor[8] observed that the magnitude of heterogeneous effects could be indexed with the term $\tau_{eb}/\tau_{sl,CO}$, which if less than 1.0, indicates evaporation of the liquid fuel occurs rapidly and emissions are controlled by quenching during mixing. The ϕ_{pz} vs unity criterion was used to determine the quench length position, as discussed earlier.

Recall that τ_{eb} is defined as the estimated time that it takes the droplet of liquid fuel with SMD to evaporate after injection into the combustor (see Fig. 2). The characteristic time that CO has resided where oxidation occurs upstream of the quench location has been designated in the l_{CO} term as $\tau_{sl,CO}$. Therefore, if τ_{eb} is greater than $\tau_{sl,CO}$ at a chosen quench location ($\tau_{eb}/\tau_{sl,CO} > 1$), the majority of the fuel has most likely not evaporated, and hence, the quench location in the calculation of $\tau_{sl,CO}$ is most likely too far upstream in the combustor.

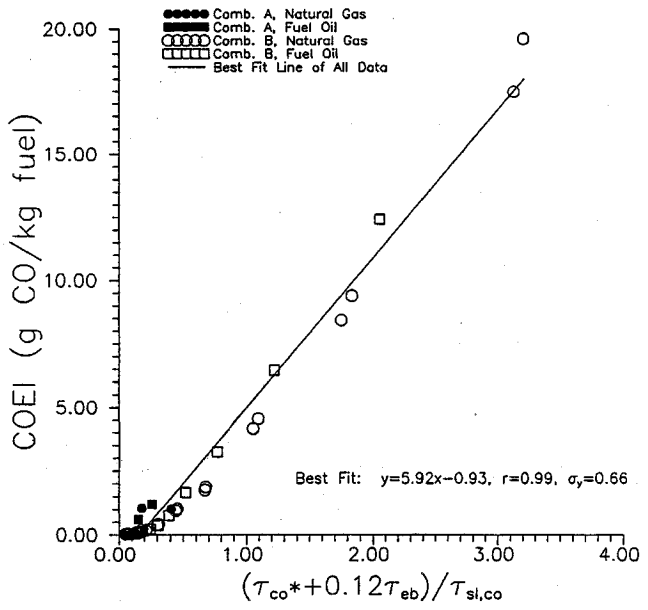

Fig. 6 Characteristic time model equation graph of combustors A and B data, without inert injection, using the new quench length algorithm with k_{CO} equal to 0.12.

Thus a new quench length algorithm is defined to select the quench length based on heterogeneous effects (if oil fired). As shown in Fig. 5, mixing times are systematically increased (via increasing the CO quenching location) until the criterion that $\tau_{eb}/\tau_{sl,CO}$ is below unity is met. The ϕ_{pz} guideline of Eqs. (10) and (11) is maintained to select either τ_{CO} or τ^*_{CO}. Note that natural gas will always have a quench length equal to l_{pri} because its value of τ_{eb} is zero.

For the present study, the Washam and Leonard rules for quench length selection have resulted in identical quench positions for the gas and oil at any given load. This result follows because both combustors maintain the same fuel and airflow rates for a certain power level independent of fuel type and both rules use equivalence ratio as a parameter. In contrast, the new algorithm of Fig. 5 systematically defines a quench length that is a function of atomization and fuel volatility through τ_{eb}.

With the new algorithm it was expected that the fuel-oil and natural-gas data alignment could be improved over that in Fig. 3, by choice of k_{CO} in

$$\text{COEI} = m(\tau^*_{CO} + k_{CO}\tau_{eb})/\tau_{sl,CO} + b \tag{12}$$

Figure 6 is a characteristic time model equation graph with the new algorithm, and an optimum value for k_{co} of 0.12 is found. This correlation is the best achieved with combustors A and B data, as the correlation coefficient is almost unity, at 0.99, and the standard deviation is 0.66 g/kg (approximately 13 ppmvd at 15% O_2). However, the magnitude of the y-intercept exceeds the standard deviation. As a result of this correlation, the CTM for CO using the new algorithm for quench length shown in Fig. 5 is

$$\text{COEI} = 5.92\,\frac{(\tau^*_{CO} + 0.12\tau_{eb})}{\tau_{sl,CO}} - 0.93, \text{ g/kg} \tag{13}$$

Conclusions

The characteristic time model was used to correlate and predict CO emissions from two heavy-duty power-generation gas-turbine engines operating on natural gas or no. 2 fuel oil without inert injection. The CTM provided only marginally acceptable predictions, as expected, since it was developed primarily with aircraft engine data. The characteristic time model was modified in view of differences between transportation and stationary engine operation. A new quench length algorithm that is more germane to the representations of global combustor physics included in the CTM was developed, and the kinetics of CO oxidation was described in more detail. The revised characteristic time model produced improved correlations of all data (±13 ppmvd at 15% O_2).

Acknowledgments

The authors appreciate funding from the Thermal Research Center of ENEL s.p.a. (the major Italian power utility), Pisa, Italy, and from CISE s.p.a. (Center for Information, Studies and Experiments), Milan, Italy, under Technical Specification DSM-ST-92-004/Purchase Order 86073. We are grateful to Max De Carli for his cooperation during the program.

References

[1]Hung, W. S. Y., "A Predictive NO_x Monitoring System for Gas Turbines," American Society of Mechanical Engineers, Paper 91-GT-306, June 1991.

[2]Tuttle, J. H., Colket, M. B., Bilger, R. W., and Mellor, A. M., "Characteristic Times for Combustion and Pollutant Formation in Spray Combustion," *16th International Symposium on Combustion*, The Combustion Inst., Pittsburgh, PA, 1976, pp. 209–219.

[3]Newburry, D. M., and Mellor, A. M., "Semi-Empirical Predictions and Correlations of NO_x Emissions from Utility Combustion Turbines," American Society of Mechanical Engineers, Paper 95-GT-70, June 1995.

[4]Newburry, D. M., and Mellor, A. M., "Semi-Empirical Correlation of NO_x Emissions from Combustion Turbines with Water/Steam Injection," American Society of Mechanical Engineers, Paper 95-GT-66, June 1995.

[5]Reynolds, W. C., "STANJAN Version 3.93," Dept. of Mechanical Engineering, Stanford Univ., Stanford, CA, 1987.

[6]Godsave, G. A. E., "Studies on the Combustion of Drops in a Fuel Spray—the Burning of Single Drops of Fuel," *4th International Symposium on Combustion*, Williams and Wilkins, Baltimore, MD, 1952, pp. 818–830.

[7]Frössling, N., "On the Evaporation of Falling Droplets," *Gerlands Beitrage sur Geophysik*, Vol. 52, Feb. 1938, pp. 170–216.

[8]Leonard, P. A., and Mellor, A. M., "Correlation of Gas Turbine Combustor Efficiency," *Journal of Energy*, Vol. 7, No. 6, pp. 556–602.

[9]Elkotb, M. M., El-Sayed Mahdy, M. A., and Montaser, M. E., "Investigation of Externally Mixing Air Blast Atomizers," *Proceedings of the 2nd International Conference on Liquid Atomization and Sprays*, Univ. of Wisconsin, Madison, WI, 1982, pp. 107–115.

[10]Lefebvre, A. H., *Atomization and Sprays*, Hemisphere, New York, 1989.

[11]Verkamp, F. J., Verdouw, A. J., and Tomlinson, J. G., "Impact of Emission Regulations on Future Gas Turbine Engine Combustors," *Journal of Aircraft*, Vol. 11, No. 6, 1974, pp. 340–344.

[12]Vogel, R. E., Troth, D. L., and Verdouw, A. J., "Fuel Character Effects on Current High Pressure Ratio, Can Type Turbine Combustion Systems," U.S. Air Force Aeropropulsion Lab., AFAPL-TR-79-2072, Environmental Sciences Lab., ESL-TR-79-29, April 1980.

[13]Gleason, C. C., Oller, T. L., Shayeson, M. W., and Bahr, D. W., "Evaluation of Fuel Character Effects on F101 Engine Combustion System," U.S. Air Force Aeropropulsion Lab., AFAPL-TR-79-2018, June 1979.

[14]Nelson, A. W., private communication to R. Munt, Pratt and Whitney Aircraft, Environmental Protection Agency, Oct. 1976.

[15]Mellor, A. M., and Ferguson, C. R., "Practical Problems in Turbulent Reacting Flows," *Turbulent Reacting Flows*, Springer–Verlag, New York, 1980, pp. 48–55.

[16]Mellor, A. M., "Characteristic Time Emissions Correlations and Sample Optimization: GT-309 Gas Turbine Combustor," *Journal of Energy*, Vol. 1, No. 4, pp. 244–249.

[17]Mellor, A. M., "Characteristic Time Emissions Correlations: the T-63 Helicopter Gas Turbine Combustor," *Journal of Energy*, Vol. 1, No. 4, pp. 257–262.

[18]Mellor, A. M., and Washam, R. M., "Characteristic Time Correlations of Pollutant Emissions from an Annular Gas Turbine Combustor," *Journal of Energy*, Vol. 3, No. 4, pp. 250–253.

[19]Prior, R. C., Tallio, K. V., and Mellor, A. M., "Turbulent Mixing and Atomization in a Confined Shear Layer," *Journal of Propulsion and Power*, Vol. 7, No. 4, 1991, pp. 488–496.

[20]Hosokawa, S., Ikeda, Y., and Nakajima, T., "Vortex Shedding Flow Calculation Using a Time-Dependent k-ε Turbulence Model," AIAA Paper 93-0020, Jan. 1993.

[21]Ikeda, Y., private communication, Kobe Univ., Kobe, Japan, July 10, 1995.

[22]Mellor, A. M., "Gas Turbine Engine Pollution," *Progress in Energy and Combustion Science*, Vol. 1, Aug. 1976, pp. 111–133.

[23]Connors, C. S., Barnes, J. C., and Mellor, A. M., "Semi-Empirical Predictions and Correlations of CO Emissions from Utility Combustion Turbines," AIAA Paper 95-2996, July 1995.

[24]Lefebvre, A. H., "Influence of Fuel Properties on Gas Turbine Combustion Performance," U.S. Air Force Wright Aeronautical Labs., TR-84-2104, Jan. 1985.

[25]Rizk, N. K., and Mongia, H. C., "Semi-Analytical Correlations for NO_x, CO, and UHC Emissions," American Society of Mechanical Engineers, Paper 92-GT-130, June 1992.